A CONTINUOUS LATE HOLOCENE RECORD OF PALEOCLIMATE CHANGE FROM GRINNELL LAKE SEDIMENT CORES, GLACIER NATIONAL PARK, MONTANA

By

Jonathan Griffith

******

Bachelor of Science

Department of Geology

Union College

March 2011

Griffith, Jonathan G., *A continuous Late Holocene record of paleoclimate change from Grinnell Lake sediment cores, Glacier National Park, Montana*. Department of Geology, Union College, Schenectady, New York, March 2011.

Grinnell Lake is a glacially-fed alpine lake in the northern Rocky Mountains of Montana. Limnological parameters and radiocarbon ages from a ~1.17 -meter-long sediment core from Grinnell Lake provide a ~1,200 year-long climate record. The objective of this thesis is to develop a multi-proxy record of glaciation by distinguishing periods of positive and negative mass balance chronologically. Two overlapping sediment cores (1P-1B-1 and 1C-2B-1) were described, photographed, and sampled at 0.5 cm, 1 cm, and 5 cm intervals and analyzed for % organic carbon, % inorganic carbon, mineral composition, bulk density, biogenic silica, and clastic sediment flux. Glacial fluctuations were identified based on downcore plots of these parameters, and correlated with previously constructed glacial and climate records from the Canadian Rockies. The results indicate that cold conditions ~1100 AD initiated the "Little Ice Age" and the expansion of the Grinnell Glacier. A warmer climate persisted from ~1120-1450 AD however two or three periods of glacial advance are possible during this time period. A subsequent cold climate ~1450-1900 AD coupled with increased precipitation ~1600-1900 AD initiated significant ice expansion reaching its maximum extent ~1900 AD. Anomalously high 20th century temperatures resulted in rapid glacial recession and mark the end of the "Little Ice Age". These results contribute to existing climate records from the Little Ice Age period and will help to analyze small scale forcing mechanisms driving climate change and how these changes might spread globally.

ACKNOWLEDGEMENTS

I would like to the Union College Geology department for its dedication and enthusiasm for undergraduate research. A sincere thanks goes to my advisor, Donald Rodbell, for all of the time he invested to my study, and the commitment and enthusiasm he always had for my project. I would also like to thank the rest of the Union College geology faculty, professor's Kurt Hollocher and David Gillikin, and lab technician Joanne Dalakos especially, for their help with data collection and interpretations. This research was made possible by the Keck Consortium, the Davenport Fellowship, and IEF funding. The Union College Geology department is special and I am thankful for the close relationships I have developed between my peers and professors. I could not be happier with my decision to pursue a degree in geology at Union College, it has been an amazing four years.

TABLE OF CONTENTS

List of Figures

List of Tables

Introduction 1.1

Glaciers are sensitive indicators of climate change, waxing and waning in response to changes in temperature and precipitation; therefore, glacial fluctuations of the past recorded in glacial deposits preserve information about the Earth's climatic history (Benn and Evans, 1998). The distribution of glaciers is primarily controlled by the interaction of precipitation, temperature and topography. Precipitation, in the form of snow, is the most important input to glaciers and will accumulate and survive provided that the amount of energy available to melt snow is low enough (Benn and Evans, 1998). The difference between a glaciers gains and losses over a given time period may be referred to as mass balance and is positive if a glacier is gaining mass (accumulation) and negative if it is losing mass (ablation). It is characteristic for mid-latitude glaciers to have marked seasonal variations in temperature resulting in distinct winter accumulation, when most precipitation falls as snow, and summer ablation, when melting predominates over accumulation and much of the precipitation falls as rain (Benn and Evans, 1998). However, glacial reconstructions cannot be directly translated into quantitative measures of temperature and precipitation (Luckman, 2000). Periods of positive mass balance can be attributed to declining temperatures, increased precipitation or some specific combination of both.

Glaciers flow in response to fluctuations in accumulation and ablation, transferring mass from upglacier regions to downglacier localities to maintain a steady state (Benn and Evans, 1998). It is important to note that due to the variable rates of accumulation and ablation, glacier flow is fastest in humid, maritime settings, and slowest in arid cold climates (Benn and Evans, 1998; Dowdeswell et al., 2010). In addition, water generated from precipitation and melting at the ice-bedrock contact can decrease the frictional force between the two masses thus resulting in

faster glacial flow rates and greater bedrock abrasion (e.g. Ostrem, 1975; Hasnain, 1996). Hallet et al. (1996) compiled all available field data on sediment yield by glaciers and found that sediment yields expressed as effective rates of glacial erosion vary from 0.001 mm yr^{-1} for cold-based polar glaciers to 10-100 mm yr^{-1} for high-activity, warm-based glaciers in southeastern Alaska. Mass balance is therefore an important control between climatic inputs and glacial behavior and as a result, past climates can be reconstructed from historical and geological evidence of glacier fluctuations.

1.2 Climate and Glacial Reconstruction Methods

Glacial records of the Rocky Mountain region, Northwest United States, have largely been established through the mapping of moraines and radiometric dating of organic material. However, moraines tend to provide ages of maximum glacial extent because each less extensive advance is subsequently destroyed by each more extensive advance (Seltzer et al., 1995; Tonry, 2010). Thus, glacial reconstructions based on moraine records are discontinuous and commonly poorly dated.

Despite alternative methods for deriving glacial records, information on glacial history between maximum ice stands, potentially constituting a large amount of time during the Holocene, is difficult to collect from surficial deposits (Leonard, 1986). The development of Pleistocene marine oxygen isotopes has been useful in interpreting conditions between maximum Pleistocene ice advances but has proven less useful in reconstructing the small glacial fluctuations of the Holocene (Leonard, 1986). However, recent climate reconstructions derived from tree-rings provides evidence of regional climate variability over the last millennium (Luckman, 2000).

These reconstructions preserve important information for distinguishing glacial advances related to reduced summer temperatures, increased precipitation, or a combination of both.

Until recently, our understanding of Holocene glacial history has been largely based on the discontinuous moraine record (Leonard, 1986) however, recent studies have interpreted variations in glacial extent from proglacial lake sediments suggesting that they might be used as indicators of upvalley glacial activity capable of providing continuous records of glaciations, recording advances, retreats, and maximum ice extents (Rosenbaum and Reynolds, 2004). Interpreting downvalley lacustrine sediments is difficult because of a lack of understanding of the relationship between glacial activity and downvalley sedimentation. Glacial sediments can at times be sequestered subglacially and at other times be flushed from storage by high runoff events (Rosenbaum and Reynolds, 2004).

Despite potential issues reconstructing glacial records based on downvalley sedimentation rates, several principle relationships have been identified. Glaciolacustrine core analyses (Leonard, 1985, 1986) suggest that annual variations in proglacial sedimentation rates are due to seasonal ablation rates (summer temperatures), while increased sedimentation rates over timespans of decades reflect either increased ice extent, periods of rapid ice recession, or both. Leonard (1986) concluded that over timespans of a century or more, sedimentation rates are directly related to changes in upvalley ice extent. The relationship between glacial extent and sedimentation rates can be complicated by the fluvial reworking of surficial deposits affecting changes in sediment availability resulting in high sedimentation rates may persist for nearly 100 years after maximum ice stands (Leonard, 1985). These paraglacial processes are thought to limit the resolution of glacial chronologies to about a century (Church and Ryder, 1972). These findings are supported by studies by Rosenbaum and Heil (1998) on Bear Lake, Utah and Idaho,

and Rosenbaum and Reynold (2004) on Upper Klamath Lake, Oregon, who found the timing of maximum glacial extent to be coeval based on glaciagenic material in lake sediments. The timing also coincides with widespread glaciations in the Rocky Mountains as modeled by radiocarbon ages (Rosenbaum and Heil, 1998).

Studies completed by W. Karlen (1981) suggest that there is an inverse relationship between clastic sedimentation rate and organic content of sediments Karlen (1981) interpreted changes in organic content as indicators for changes in upvalley glacier extent suggesting that an increase of glacial debris in the water column results in lower organic production. C/N ratios can be used to distinguish algal and terrestrial-plant origins of organic matter in lake sediments (Sharp, 2007). Low C/N ratios in aquatic plants can be attributed to an absence of cellulose and lignin, in contrast to terrestrial plants, who fight the effects of gravity with lignocellulosic structural polymers and are therefore carbon rich (Sharp, 2007). Variations in C/N ratios in a sediment core from the northern basin of Lake Baikal, southern Siberia may be related to a change in sediment type. Qui et al. (1993) concluded that increases in glacially derived meltwater and the resulting influx of terrestrial minerals lowered productivity and decreased biogenic silica concentrations. Additional studies by Bradbury et al. (1994) on Lake Baikal support this conclusion attributing a lack of diatoms in the lake to excessive turbidity from glacial meltwater entering the lake and impeding productivity.

1.3 Review of late Pleistocene-Holocene Climate

Northern Hemisphere paleotemperature reconstructions from Greenland ice cores provide a continuous and detailed record of high latitude climate variability throughout the past 50,000 yr B.P. Alley et al. (1993) used the Greenland ice core (GISP2) to show a sequence of late

Pleistocene polar climatic periods. First, a pronounced warm period known as the Boiling/Allerod (B/A) inerstadial occurred approximately 14.5-12.9 kyr B.P. This ended abruptly with the onset of the Younger Dryas (YD) cold interval (12.9-11.5 kyr B.P.), where Greenland summit temperatures are estimated to have rapidly decreased to ~15^{o}C below modern temperatures (Alley, 2000). The YD was succeeded by the rapid onset of the Preboreal warm interval (11.5 kyr B.P.), which marked the beginning of the Holocene.

There is substantial evidence for glaciations in the western United States during the Younger Dryas. Dated moraine records suggest glacial advances in the Colorado Front Range (13.1-11.3 ka), the Wind River Mountains (12.6 ka), and the Canadian Rocky Mountains (13.2-11.6 ka) indicating widespread glaciation throughout the Rocky Mountains during the Younger Dryas (Licciardi et al., 2004). These data are consistent with other glacial records from the southern Coast Mountains of British Columbia, the North Cascades, and the San Vernardino Mountains of southern California. However, dated lacustrine sediments near Mount Rainier, Washington, and in the Sierra Nevada document the absence of Younger Dryas glaciations. Licciardi et al. (2004) suggest that glacial systems in these two regions may be sensitive to changes in precipitation and attribute the absence of glaciations at Mount Rainier and in the Sierra Nevada to reflect negative regional precipitation anomalies. Lacustrine sediments from Elbow Lake in the Uinta Mountains, Utah, display values of measured proxies that are consistent with a cold and dry environment during the Younger Dryas. Low water temperatures and prolonged ice cover inhibited primary productivity resulting in low LOI and bSi values. Dry conditions limited the input of terrestrial organic matter and clastic debris, resulting in low C/N values and low grain size (Corbett and Munroe, 2010).

With the exception of a brief stadial ~9.2- and 8 kyr B.P., climatic conditions throughout the Holocene were much more constant than the Pleistocene. Palynological and macrofossil evidence from the northwestern United States and western Canada suggest that the "Altithermal" interval (period of maximum warmth and dryness in the Holocene) occurred from 10- and 6 kyr B.P. (Davis and Osborn, 1987; Benedict, 1973). This period may have been interrupted by an interval of cooling between ~9.2- and 8 kyr B.P., possibly resulting in several small glacial advances. Luckman and Osborn (1979) suggested that the Crowfoot advance in the Canadian Rockies occurred between 9.2- and 8.7 kyr B.P. Shallow ponding and deposition of clastic sediments in a bog at the base of Satanta Peak, Colorado Front Range, Colorado, provide additional evidence for the possibility of a minor glacial advance ~8 kyr B.P (Benedict, 1973). The "Altithermal" period reach a peak of warmth and aridity between 7.5- and 6 kyr B.P. and ended with the beginning of the Triple Lakes glacial advance (Benedict, 1973). The advance is estimated to have begun 5 kyr B.P., and included up to three secondary advances concluding 3 kyr B.P. Between 3000 and 1850 B.P. an interval of soil formation records a morphological break in the morainal record which was reactivated by the advance of the Audubon glacier (1850-950 B.P) (Benedict, 1973).

1.4 Little Ice Age

The Little Ice Age is the term reserved for the most recent period of extensive glacier expansion however its timing has been subject to much debate. Fagan (2000) constrains the timing of Little Ice Age cooling period to the 16^{th}-19^{th} centuries based on evidence from Europe, whose climate was strongly impacted. This period began with a trend towards enhanced glacial conditions following the warmer medieval warm period (Medieval Climatic Optimum). A

dramatic retreat of glaciers during the 20th century marks the end of the Little Ice Age. Significant evidence (Leonard, 1985; Leonard, 1986; MacGregor et al., 2010; Carrara, 1989; Luckman, 2000; Grove, 1988) demonstrates that regions outside of Europe exhibited similar periods of cooler conditions and expanded glaciations however, the timing and extent of these fluctuations are variable and therefore the idea that the Little Ice Age was a globally synchronous cold period has been dismissed (Bradley and Jones, 1993; Mann et al., 1999). Contrary to the Pleistocene cooling events which demonstrate clear global expression by a dramatic growth of all major continental ice sheets and a lowering of global temperatures (Mann et al, 1999), the Little Ice Age does not display a continuous period of cooling or glacial conditions. Colder conditions are variable over the past thousand years, and are punctuated by intermittent periods of warmth (Leonard, 1986; Bradley and Jones, 1993).

Paleobotanic records from the Canadian Rockies suggest a transition from a warm to cold climate ~1100. Moraine evidence suggests the climate was cool enough to initiate glacial expansion. Grove (2001) radiocarbon dated fragmented material preserved in moraines and developed ring width chronologies from in situ stumps and detrital trees to show that the Robson Glacier in the Canadian Rockies was advancing between *AD* 1142 and 1150. Other types of evidence support the hypothesis of an early (12th and 13th century) initiation of the "Little Ice Age" such as variations in proglacial sedimentation rates at Hector Lake, Canada interpreted by Leonard (1986) as recording glacial advance in the 13th century.

Evaluating tree rings as proxies for climate variability allows scientists to attribute glacial fluctuations to specific climatic events. Luckman (2000) determined that most regional glacier advances in the Canadian Rockies follow periods of reduced summer temperatures, reconstructed from tree rings ca. *AD* 1190-1250, 1420-1500, 1690s and the 1800s. Precipitation rates can also

be reconstructed using tree rings. Luckman (2000) found that glacial advances in the early 1700s, the late 1800s, reflect both increased precipitation and reduced summer temperatures. The "Little Ice Age" continued until the mid-19th century when a warming climate initiated glacier retreat (Key et al., 2009).

The advance and retreat of glaciers progressed at variable rates in response to the Little Ice Age and subsequent warming. Data from the Canadian Rockies suggest that the expansion of glaciers early in the "Little Ice Age" was much slower than regional advances in 18th and 19th centuries (Grove, 2001). This finding is consistent with Leonard's (1986) study on Hector Lake in which he used sedimentation rate as a proxy for upvalley glacial extent. Leonard determined that latter period of glaciation was more significant because sedimentation rates were much higher than during the 13th century advance.

Likewise, the degree of glacial recession in Glacier National Park, Montana has varied among different glaciers over time (Fig. 1). For example, during the period of *AD* 1859 to 1920, the average recession of the Grinnell Glacier was about 6 m a^{-1} (Key et al., 2009). From *AD* 1920 to 1946 the Grinnell Glacier experienced the largest retreat of any glacier in Glacier National Park with an average recession rate of 15 m a^{-1} (Key et al., 2009). Between 1946 and 1979, recession averaged about 4 m a^{-1} reducing the glacier to 41% of its former area (Key et al., 2009). The retreat of glaciers observed in Glacier National Parks is consistent with trends in temperate glaciers in other regions over the last 150 years (Key et al., 2009).

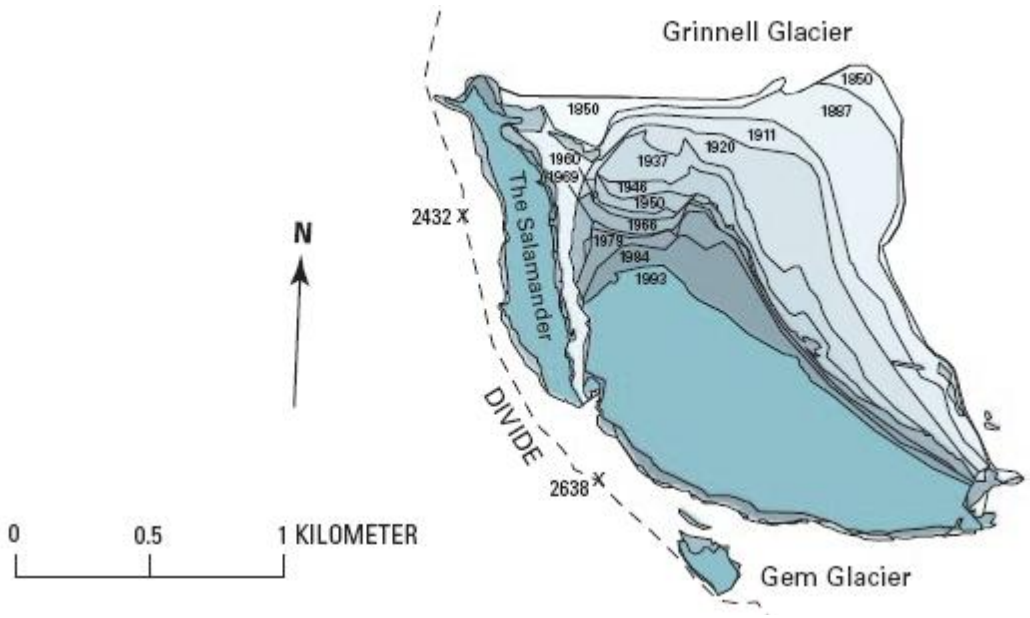

Figure 1. Little Ice Age recession chronology of the Grinnell Glacier. The glacier was first mapped in 1900; prior reconstructions are based on photographs taken by early explorers. From 1887 to 1979, the glacier was reduced to 41% of its former area (Figure from Key et al., 2002).

Objectives

The objective of this study is to reconstruct a climate history of Glacier National Park, Montana from geological evidence of glacier fluctuations preserved in a proglacial lake. To accomplish this goal, I will examine a ~900 year-long sediment core from Grinnell Lake and investigate the relationship between climate, glacial activity, and the subsequent development and transport of clastic and organic material. Ultimately, I hope to develop a record of clastic sediment flux that can be used as a proxy indicator of glaciations and of climatically-driven changes in sedimentation to alpine lakes in the Rocky Mountains.

STUDY SITE

Grinnell Lake is located east of the Continental Divide in Glacier National Park, Montana (Figure 2). The lake is one of four in the Grinnell Glacier/Many Glacier valley and has a catchment area of about 25 km^2 that includes the Grinnell Glacier (~2000 m elevation) (MacGregor et al., in press). The lakes include Upper Grinnell Lake, Grinnell Lake (study site), Lake Josephine, and Swiftcurrent Lake (listed in order from upvalley to downvalley). The 1.17-m-long sediment core consisting of a 0.75 m surface core (LGRIN-1B-1P-1) and an additional 0.42-m-long core (LGRIN-1C-2B-1) were collected in ~20-m water depth (Fig. 3). The coring was completed away from the surrounding shorelines and downvalley from deltaic and mass wasting features.

The Grinnell Glacier valley is characterized by steep hillslopes; between Mount Grinnell and Grinnell Lake (~2 km distance) there is a 1 km change in elevation (MacGregor et al., in press). The Grinnell Glacier is bordered by a ~500-m-high headwall. A 460 m step in topography exists between Upper Grinnell Lake and Grinnell Lake over which water from Upper Grinnell Lake flows (MacGregor et al., In Press). Relief in the basin diminishes by approximately 30 m downvalley.

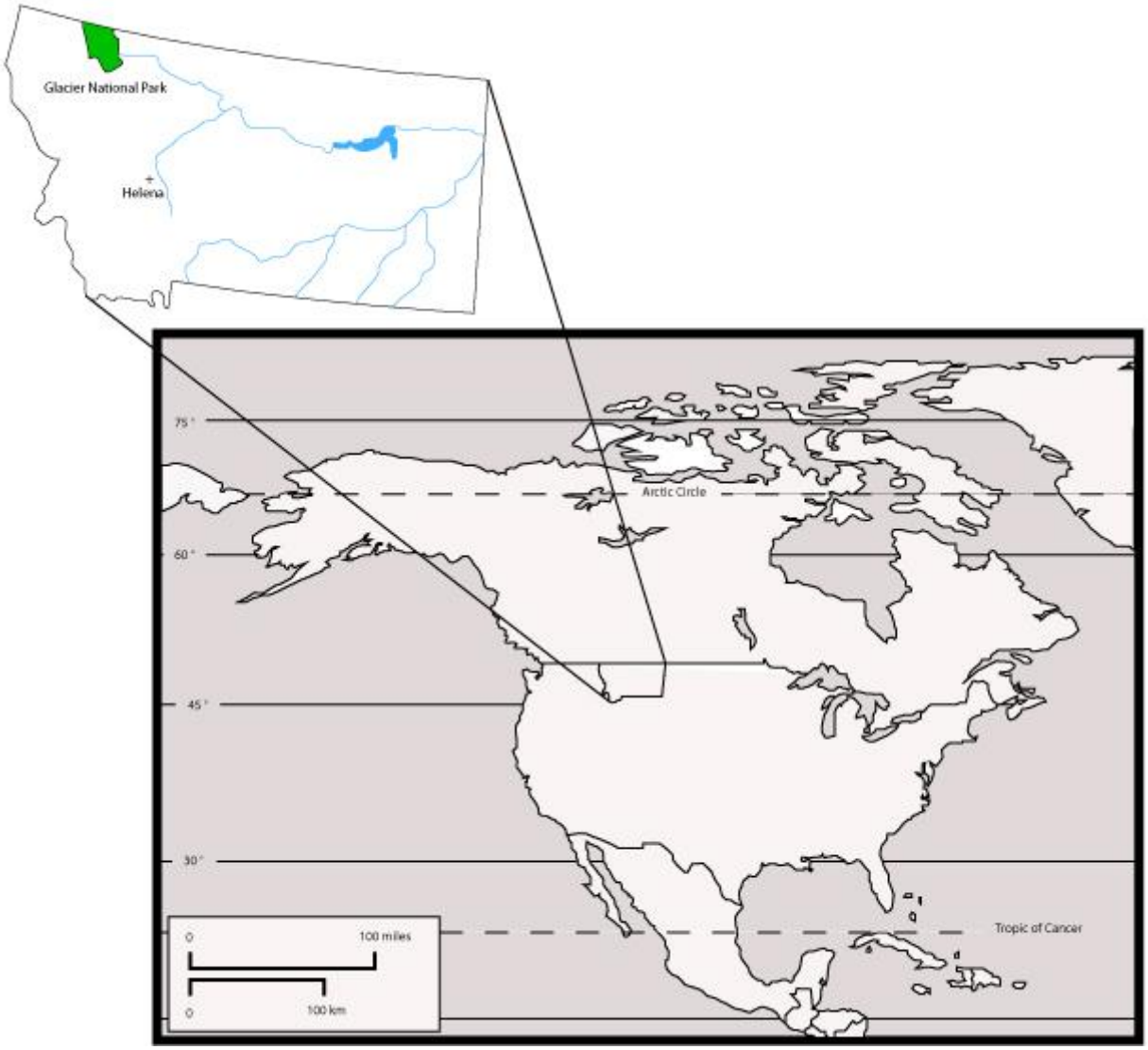

Figure 3. Location map of Montana in the United States. Inset shows the position of Glacier National Park with respect to Montana.

Figure 3. Sediment within the white box from cores 1C-2B-1 (left) and 1B-1P-1 (middle) was used to get a continuous 1.17 cm sediment core.

GEOLOGIC SETTING

The Grinnell Lake drainage basin is underlain by sedimentary rocks of the Middle Proterozoic Belt Supergroup ranging from about 1,600 Ma to 800 Ma (Carrara, 1989). The Supergroup consists of largely argillaceous, arenaceous, and calcareous strata indicative of subtidal, intertidal, and alluvial depositional environments and is about 2.9 km thick (Table 1; Horodyski, 1983). Grinnell Glacier is currently eroding the stromatolitic Siyeh Limestone of the Helena Formation (Fig. 4; MacGregor et al., In Press). The Siyeh Limestone consists of dolomitic limestone, dolomitic and calcitic argillite, and dolomitic and calcitic sandstone (Horodyski, 1983) and is the only source of dolomite in the valley (MacGregor et al., In Press).

Table 1: Stratigraphy and lithology of the Middle Proterozoic Belt Supergroup. The Grinnell Glacier currently erodes into the Siyeh Limestone (table modified from Horodyski, 1983).

Formation	Thickness (m)	Rock Description
Siyeh Limestone	780	Gray, muddy and sandy dolomitic limestone, dolomitic and calcareous argillite and muddy sandstone; minor oolitic limestone
Grinnell Argillite	606	Red argillite and sandy argillite; subordinate green argillite, sandy argillite, and quartzose sandstone
Appekunny Argillite	700	Green argillite and sandy argillite; quartzose sandstone locally prominent; minor black mudstone
Altyn Limestone	>150	Gray silty and sandy dolostone

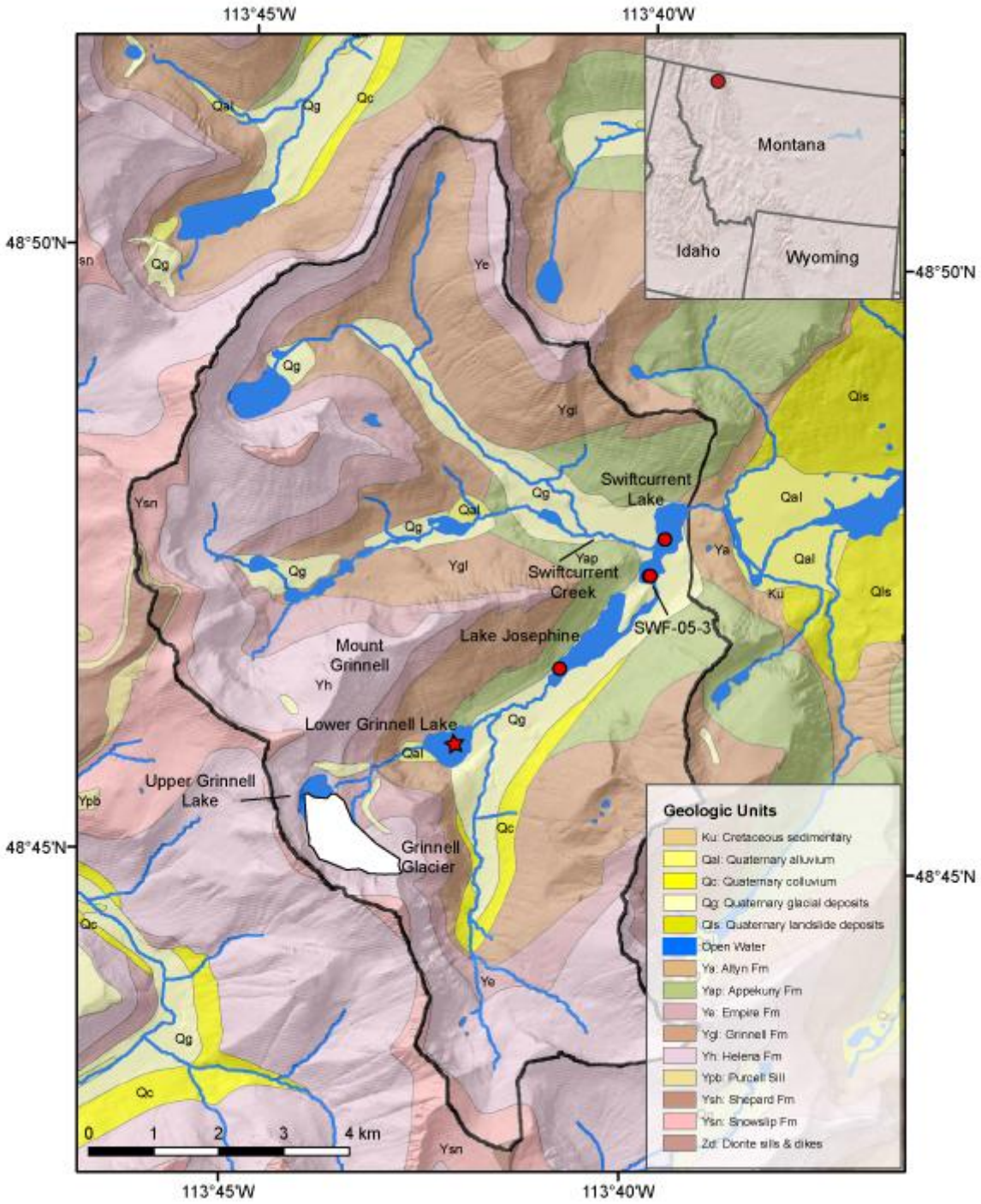

Figure 4. Bedrock geology map of the Many Glacier region of Glacier National Park, including Grinnell Glacier, Upper Grinnell Lake, Grinnell Lake (red star), and downvalley lakes. The Grinnell Glacier is underlain by the Siyeh Limestone of the Helena Formation.

CLIMATE

The continental divide separates Glacier National Park into two areas dominated by different climactic systems (Carrara, 1989). The area west of the Continental Divide is primarily controlled by Pacific air masses and constitutes the wettest part of Montana. Exceptions to this occur during the winter when cold continental polar air masses from Canada descend from the mountains into the region. And occasionally during the spring and summer, warm moist air masses from the Gulf of Mexico occupy this area (Carrara, 1989).

The area east of the Continental Divide (study site location) is dominated by cold, dry continental-polar air masses during the winter resulting in diminished precipitation (Carrara, 1989). Winter winds commonly exceed 160 km/hr due to an invasion of Pacific air masses which, having lost their moisture ascending the western slopes of the Continental Divide, rapidly descend the eastern slopes. Following the northward retreat of the polar front in the spring, air masses from the Gulf of Mexico invade the region resulting in increased precipitation from April through June (Carrara, 1989).

Climate data collected from the Kalispell-Glacier Park International Airport station (~69 km from Grinnell Glacier, elevation difference of -1232 m relative to Grinnell Lake; Google Earth) from July 1996 – December 2008 indicate that temperatures are frigid and strongly seasonal and that precipitation data classifies this climate as semiarid and weakly seasonal (Fig. 5). Climate classifications were determined following the scheme produced by Ritter et al. (2002).

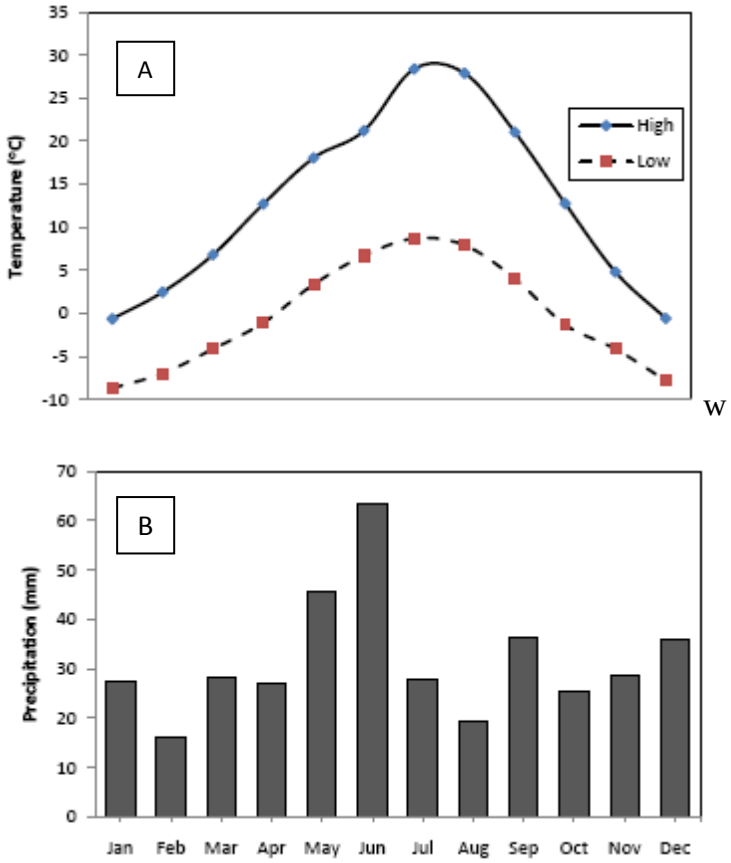

Figure 5. Mean monthly high and low temperature (A) and mean monthly precipitation (B) data collected between 1996-2008 from the Kalispell-Glacier International Airport, MT, ~69 km southwest of the study site.

METHODS

Cores LGRIN10-1B-1P-1 and LGRIN10-1C-2B-1 were collected in July 2010 using a Bolivian-type corer. The cores were logged, split, photographed, tested for magnetic susceptibility, and described using smear slides at the University of Minnesota's LacCore lab. The cores were subsampled at constant intervals and mailed to Union College where analytical measurements including x-ray diffraction (XRD) and carbon coulometry were conducted. A third core was collected using a gravity surface corer. This core was extruded on site at 0.5-cm resolution and used for lead-210 dating.

Carbon coulometric analyses were completed at Union College's core lab. Analysis of total carbon (TC) was conducted using a CM 5200 Autosampler Furnace at 0.5-cm spacing until a depth of 50 cm core and at 1-cm interval continuously thereafter. Samples for TC were combusted in oxygen at 1000^{o}C to convert organic and inorganic forms of carbon to CO_2. The CO_2 released was measured with a UIC coulometer.

Analysis of total inorganic carbon (TIC) was conducted using a CM 5230 TIC, the same sampling procedures followed for TC analyses were applied to the TIC analyses. Inorganic carbon was determined by measuring the CO_2 released after the samples were acidified in 2N $HCl0_4$. Total organic carbon was determined by subtracting TIC from TC: TOC=TC-TIC.

Carbon and nitrogen isotopic analyses were completed at 5-cm increments throughout the length of the core. A small sample, ~4-5 mg, was placed in a silver cup and several drops of HCl were added to the sample prior to enclosing the cup. Samples were sent to the University of Iowa and run on a Finnigan MAT Delta Plus XL mass spectrometer in continuous flow mode connected to a Costech Elemental Analyzer, and C and N were measured as peak areas. Six reference standards (three Sucrose and three acetanilide) were used for isotopic corrections, and to assign the appropriate isotopic scale. Acetinilide standards were used to generate a peak area plot and trendline. Carbon and nitrogen peak area data were substituted into the trendline equation to calculate the mass of carbon and nitrogen in the original samples. C/N values were produced by dividing mass percent carbon by mass percent nitrogen.

Silica components in sediment can be separated between diatoms, sponge spicules, and silicate minerals (Conley and Schelske, 1992) by step-wise dissolution because dissolution rates of siliceous components vary in a strong basic solution. For ~48 selected samples, collected longitudinally every 5 cm from the sediment cores, were analyzed for biogenic silica (bSi)

following the extraction technique outlined in DeMaster (1981). Details of analytical procedures are available at: <http://www1.uni-on.edu/~rodbelld/CoreLab.html>. Samples were analyzed for dissolved silica (DSi) by Intra-Coupled-Plasma Mass Spectroscopy (ICPMS). BSi is determined by regression analysis on the increase of DSi concentration with time and then extrapolation back to the y intercept to determine the bSi in the sediment sample (Conley and Schelske, 1992). The y-intercept represents the wt % bSi relative to the original sample mass. These data were used to calculate the flux of clastic sediment ($Flux_{clastic}$) from:

$Flux_{clastic} = SR(BD - ((BD \times TOM) + (BD \times bSi))$

Where SR is the bulk sedimentation rate (cm yr^{-1}), BD the bulk density (g cm^{-3}), TOM the weight fraction organic matter of the bulk sediment, and bSi the weight fraction of biogenic silica in the sample. TOM was calculated from TOC (%)/44 to reflect the molar ratio between plant cellulose $(C_6H_{10}O_5)n$ and TOC (%) (Rodbell et al., 2008).

To develop a chronology, terrestrial material was extracted from the core at cumulative depths of 65 cm (wood fragment) and 90 cm (organic matter) to be radiocarbon dated. The basis of radiocarbon dating is that the decay rate of the unstable carbon isotope, ^{14}C, is invariable so that a given quantity of ^{14}C will decay to its daughter product, nitrogen, in a known interval of time (Bradley, 1985). Thus, the measurement of ^{14}C concentration today will reveal the amount of time that has elapsed since the sample was emplaced. Radiocarbon (^{14}C) is produced in the upper atmosphere by neutron bombardment of atmospheric nitrogen atoms. These radiocarbon atoms are then rapidly oxidized to $^{14}CO_2$ and mixed with the rest of the atmospheric carbon dioxide which is inevitably consumed by plants and animals through photosynthesis and respiration. The ^{14}C content of tissues in these organisms is in equilibrium with that of the atmosphere because there is a constant exchange of new CO_2 as old cells die and are replaced

(Bradley, 1989). However, once the organism dies, this exchange and replacement of ^{14}C from the atmosphere stops and the ^{14}C content of the organism declines as it decays to nitrogen.

The age of a sample dated radiometrically is determined by comparing the remaining ^{14}C fraction of a sample to that expected from atmospheric CO_2. Therefore, it is necessary to know the concentration of atmospheric $^{14}CO_2$ at the time the sample died. From the study of tree rings, it has become clear that the rate of radiocarbon production has not been constant through time. Variability in ^{14}C concentrations may result from an assortment of factors, one being changes in the intensity of the Earth's magnetic field. A strong inverse relationship exists between ^{14}C concentration and magnetic field variations, such that a decrease in magnetic field strength (thus allowing more cosmic rays to penetrate the atmosphere) corresponds to an increase in the concentration of ^{14}C (Bradley, 1989). However, by measuring the radiocarbon age of tree rings of known age, it is possible to construct calibration datasets that may be used to convert radiocarbon ages into calibrated calendar years. It is in this way that an internationally agreed upon radiocarbon calibration dataset was developed in 1982.

The radiocarbon age of two samples was determined using CALIB 4.0. CALIB uses a calibration dataset to convert from radiocarbon age to calibrated calendar years by calculating the probability distribution of the sample's true age. The mean of this distribution was used in this study to approximate the calendar year. All calendar years are reported in "years before present" (BP), which, is the number of radiocarbon years before 1950. After 1950, the testing of nuclear weapons became a common practice throughout the world and significantly increased atmospheric ^{14}C concentrations.

DATA & INTERPRETATION

Two accelerator mass spectrometry (AMS) radiocarbon (^{14}C) dates indicate that the 1.17 meter-long lacustrine sediment core extracted from Grinnell Lake provides an ~1220 cal yr B.P.-to present lake record (Table 2). To account for the lack of dated material in the bottom of the core (below the oldest radiocarbon age of ~922 cal yr B.P. and depth of 96 cm), the average sedimentation rate of 0.069 was extrapolated to the base of the core (Fig. 6).

Table 2. AMS radiocarbon dates and calibrated ages from the Grinnell Lake sediment core.

UCIAMS #	**core**	**core depth (cm)**	**running depth (cm)**	**material**	**14C age (14C yr B.P.)**	**Calibrated Age (cal yr B.P.)**	**calculated positive error (yr)**	**calculated negative error (yr)**
84864	1B-1P-1	80-81	65	twig	385 ± 20	470	29	10
84865	1C-2B-1	72-73	96	organic matter	990 ± 20	922	12	13

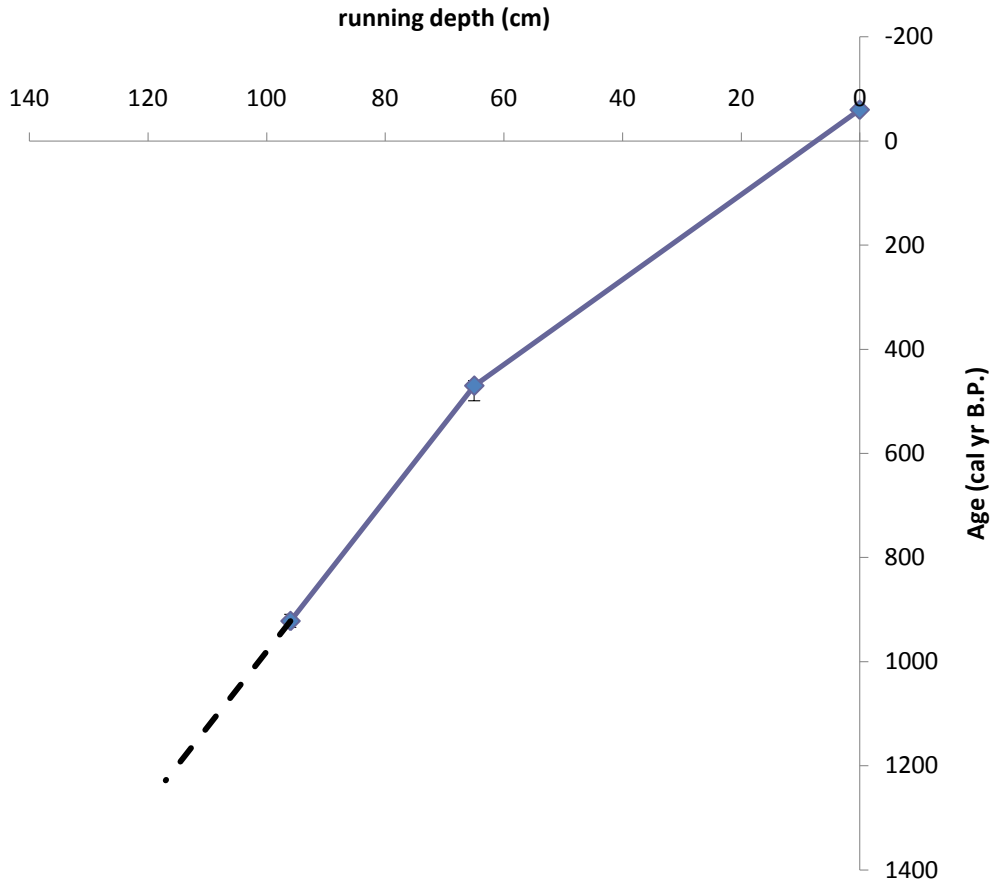

Figure 6. Age-depth model for Grinnell Lake derived from linear interpolation of AMS radiocarbon dates which were converted to calibrated calendar years (plotted in blue).

The sediment extracted through these two sediment cores (cores 1B-1P-1 & 1C-2B-1) was generally massive well-laminated mud with colors varying between light gray, gray, and dark gray. The varying color regimes in the sediment may provide evidence that could distinguish sedimentological and biological processes in the lake. Light gray layers may represent fine-grained glacial flour. In contrast, dark gray layers might be an indicator for identifying periods increased lake productivity. Two brown bands are present in the upper 3 cm of the core and are likely the result of oxidation. Distinct bands of organic debris, including

grass, woody chunks, and unidentified dark specs are also present. Clasts ranging from 0.5-6 cm in diameter were present in concentrated localities throughout the cores. The largest clasts, ~4.5 and ~ 6 cm respectively, were isolated however smaller clasts were present in bunches. The clasts exhibit clear lithologic differences and demonstrate that in addition to glacially produced sediment, hillslope processes affect the sediment delivery to the lakes. XRD data supports this finding as minerals from the siltstones, shales, limestones, and sandstones, were present in the core (Appendix 1). Complete core descriptions are compiled in the Appendices 2 and 3.

Limnological parameters and physical properties, including organic carbon, inorganic carbon, bulk density, magnetic susceptibility, clastic sediment flux and carbon isotopes, document the composition and glacial flour influx of Grinnell Lake throughout the Little Ice and past 1,200 years.

Carbon Content

Allochthonous or external source material enters lakes in various forms and is generally inversely related to organic carbon. Although lakes can be less productive during times of glacial advance, it is also important to note that autochthonous organic carbon may simply be diluted by the influx of clastic sediment in the record. All inorganic carbon deposited in Grinnell Lake was assumed to be allocthonous because the lake is fed glacial meltwater and receives precipitation throughout the year making authigenic carbon unlikely. Throughout the core set, peak inorganic carbon values are inversely related to organic carbon data. % inorganic carbon is nearly absent from the record for the first 300 years however a pronounced spike ~1090 *AD* denotes the deposition of allochthounous material (Fig. 7). Approximately ~1500 *AD* inorganic carbon values exceeded 1.5% and coincide with the lowest % organic carbon values in the

record. From ~1500-1900 *AD*, pulses of inorganic carbon are present in the record about every 90 years, with the pulses increasing in magnitude towards the surface. The greatest % inorganic carbon values exist in 1870 *AD* and 1900 *AD*. The inorganic carbon peak in 1900 *AD* denotes the last significant pulse of inorganic carbon to the lake with low inorganic carbon values persisting until today.

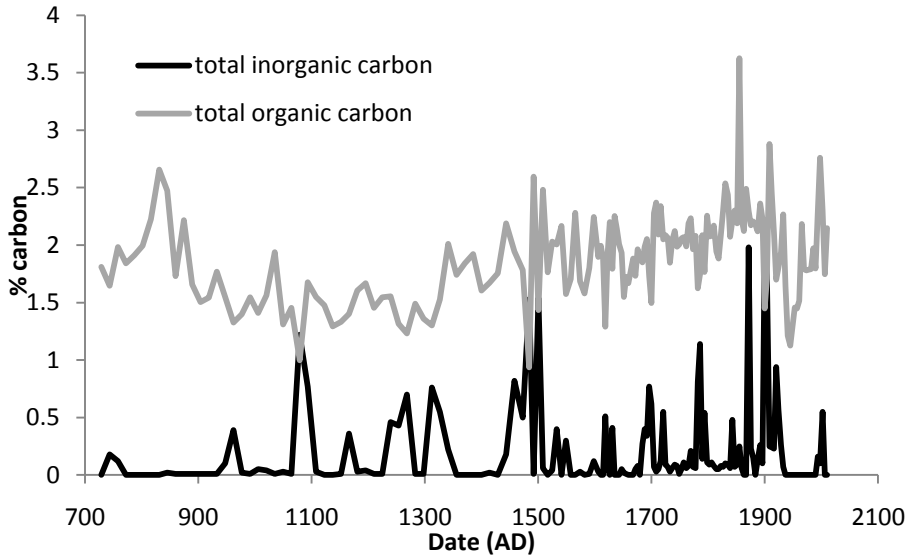

Figure 7. Plots of total inorganic carbon and organic carbon through time. Inorganic carbon peaks coincide with rapid decreases in organic carbon. Increased frequency and magnitude of inorganic carbon peaks from ~1600-1850 *AD* coincide with an overall increase in organic carbon.

Carbon and Nitrogen Isotopes

C/N ratios reflect in-lake production of organic matter, as well as the type and origin of organic material (MacGregor et al., In Press). C/N ratios of organic matter from Grinnell Lake are low ranging from 11.3 to 7.5 (Fig. 8). These values are within the range observed at Swiftcurrent Lake and indicate that organic matter was predominantly derived from

autochthonous sources (MacGregor et al., In Press; O'Reilly et al., 2003). The record is punctuated by abrupt changes however an overall decreasing trend is observed. C/N values significant decrease from ~1640-1940 *AD* where values go from 11.3 to 7.5. In contrast, $\delta^{13}C$ values display a clear increasing trend from 780 to 1860 *AD* after which $\delta^{13}C$ values shift +0.8 ‰ in 1920 *AD* (Fig. 9). $\delta^{13}C$ values range from -27.5 ‰ to -24.7 ‰. $\delta^{15}N$ values range from 0.9 ‰ to 3.8 ‰ however display no discernable trend.

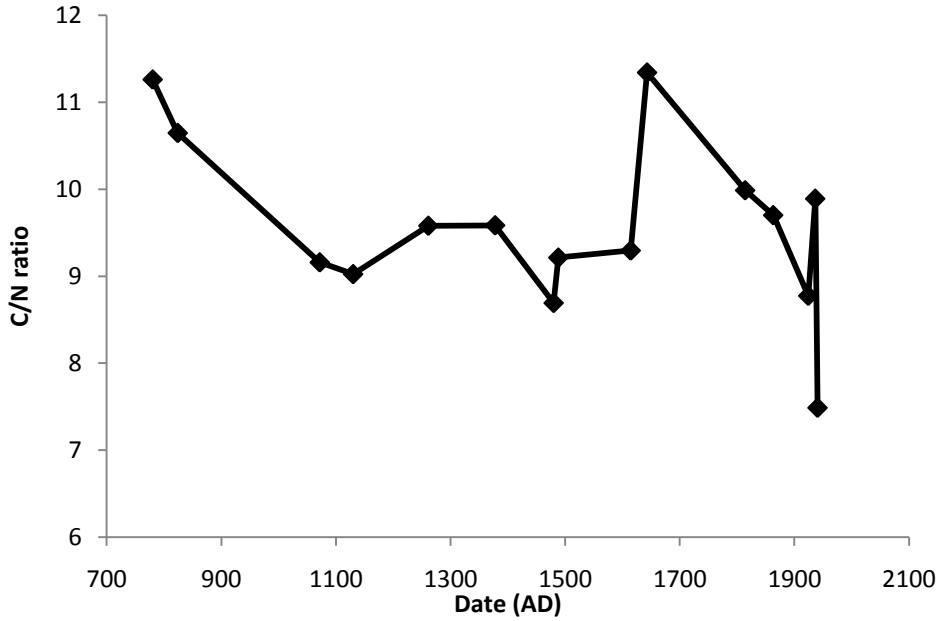

Figure 8. C/N values range from 11.3 to 7.5 and display an overall decreasing trend.

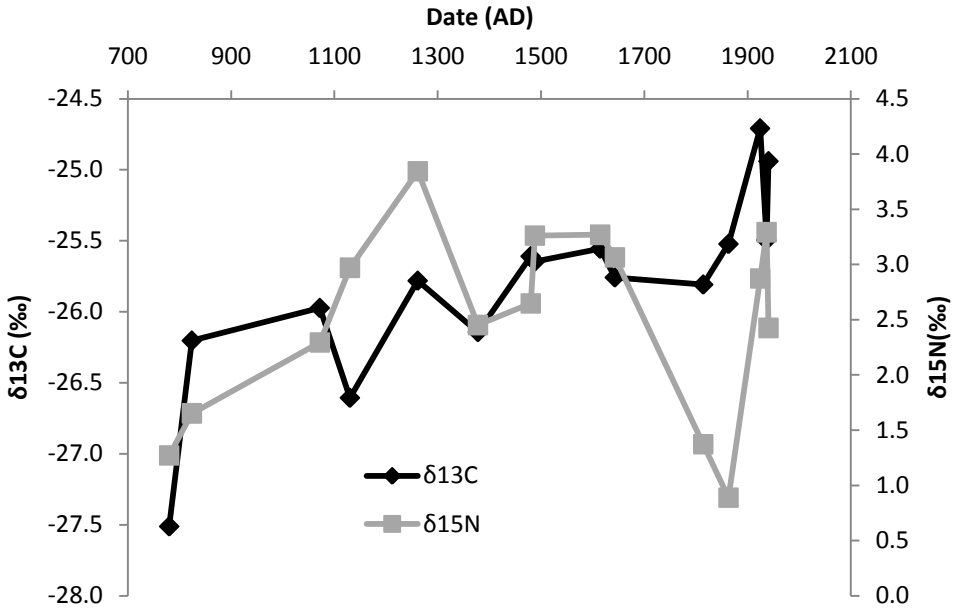

Figure 9. Plots of $\delta^{13}C$ and $\delta^{15}N$ values through time. $\delta^{13}C$ values display and increasing trend however $\delta^{15}N$ values change sporadically.

Magnetic Susceptibility

Magnetic susceptibility is a function of the composition and concentration of magnetic minerals, and, to a lesser extent, grain size (Tonry, 2010). Magnetic minerals in lake sediments are primarily detrital, therefore their abundance can be diagnostic of the relative contribution of lithogenic versus biogenic contributions to the sediment (Cohen, 2003). Peaks in magnetic susceptibility may be indicative of high glacial flour concentrations, and reflect periods of increased glacial extent. Figure 10 displays plots of magnetic susceptibility and biogenic silica through time. Similar to the relationship observed between inorganic carbon and organic carbon, MS and biogenic silica are inversely related throughout much of the core however, from ~1700-1920 *AD*, the two increase together. A rapid increase in MS ~1100 *AD* documents the input of allochthonous material to the lake. MS values decrease from 47.9 m^3/kg ~1100 *AD* to 26.3 m^3/kg ~1400 *AD*. A subtle increase in MS ~1490 *AD* is again followed by a rapid decrease. MS

values remain relatively constant at 22 m^3/kg from ~1530-1650 *AD*. From ~1650-1920 *AD*, MS values gradually increase, peaking at 35.6 m^3/kg in 1920 *AD*.

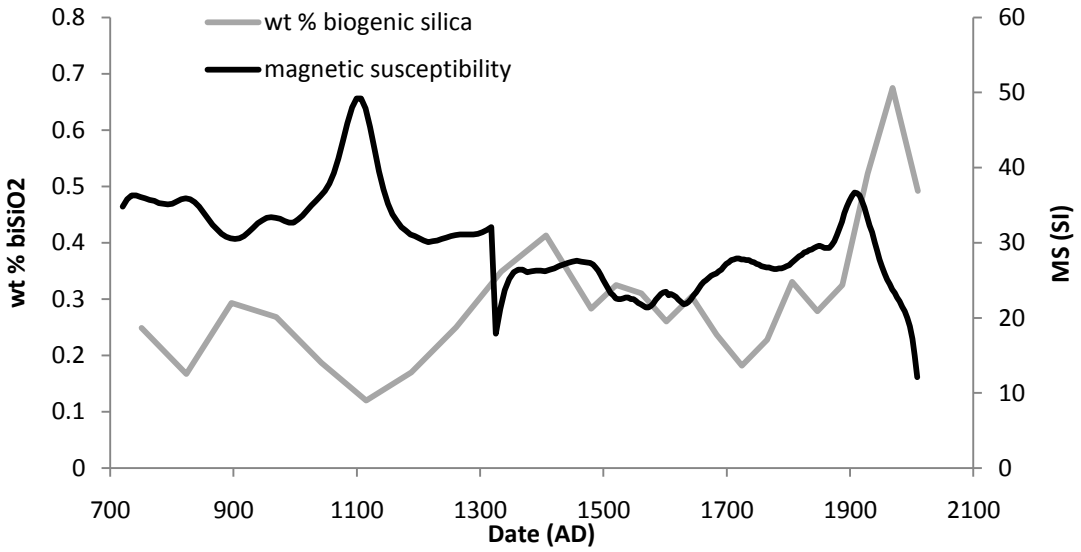

Figure 10. Plots of magnetic susceptibility and wt % biogenic silica. Plots of inversely related until ~1700 *AD* at which point they increase together.

Bulk Density & Clastic Sediment Flux

Bulk density profiles of sediment indicate hydrological changes within a lake basin, which are related to changes in ice extent. Alpine glaciers occupying the headwaters of small, high-altitude valleys are the dominant hydrological control governing sedimentation in a lake basin (Cohen, 2003). Two climatological parameters that will increase ice volume, and thus increase the volume of meltwater able to transport sediment are increased, precipitation and decreased temperature. Meltwater entrains dense sediment, such as glacial flour, thereby increasing the bulk density and magnetic susceptibility of the lacustrine sediment. Conversely, periods of reduced meltwater allow for biogenic processes to dominate a lake leading to the

accumulation of less dense organic matter. Therefore, bulk density data should track with total inorganic carbon and vary inversely with total organic carbon.

Clastic sediment flux has also been used as a proxy for interpreting ice extent with high flux measurements corresponding to increased ice extent. To acquire flux data, the biogenic material was dissolved, thus leaving behind only the dense clastic component. Therefore, clastic sediment flux, bulk density, magnetic susceptibility, and total inorganic carbon should track together and reflect the input of allocthonous minerogenic material to the lake.

Bulk density and clastic sediment flux values remain relatively stable from 740-1090 *AD* and inorganic carbon is nearly absent from the record (Fig. 11). A rapid increase in inorganic carbon at 1090 *AD* corresponds to increases in both clastic sediment flux, magnetic susceptibility, and bulk density. Clastic sediment flux values more than double from 1400-1480 *AD* and coincide with distinct peaks in both bulk density and inorganic carbon. The highest clastic sediment flux value occurs ~1550 *AD*. This increase coincides with a significant increase in bulk density but only a small increase in inorganic carbon. From 1500-1900 *AD*, overall increases in bulk density, magnetic susceptibility, % inorganic carbon, and clastic sediment flux are shown with each reaching their greatest values in ~1900 *AD*. Peak inorganic carbon values in 1870 *AD* and 1900 *AD* coincide with rapid increases in bulk density and clastic sediment flux and are interpreted to reflect the period of maximum glacial extent as well as the time immediately following deglaciation where loose material may be exposed to fluvial reworking. The sharp decline in these three proxies following the 1900 *AD* anomaly denotes the beginning of glacial recession which has continued for the past 100 years.

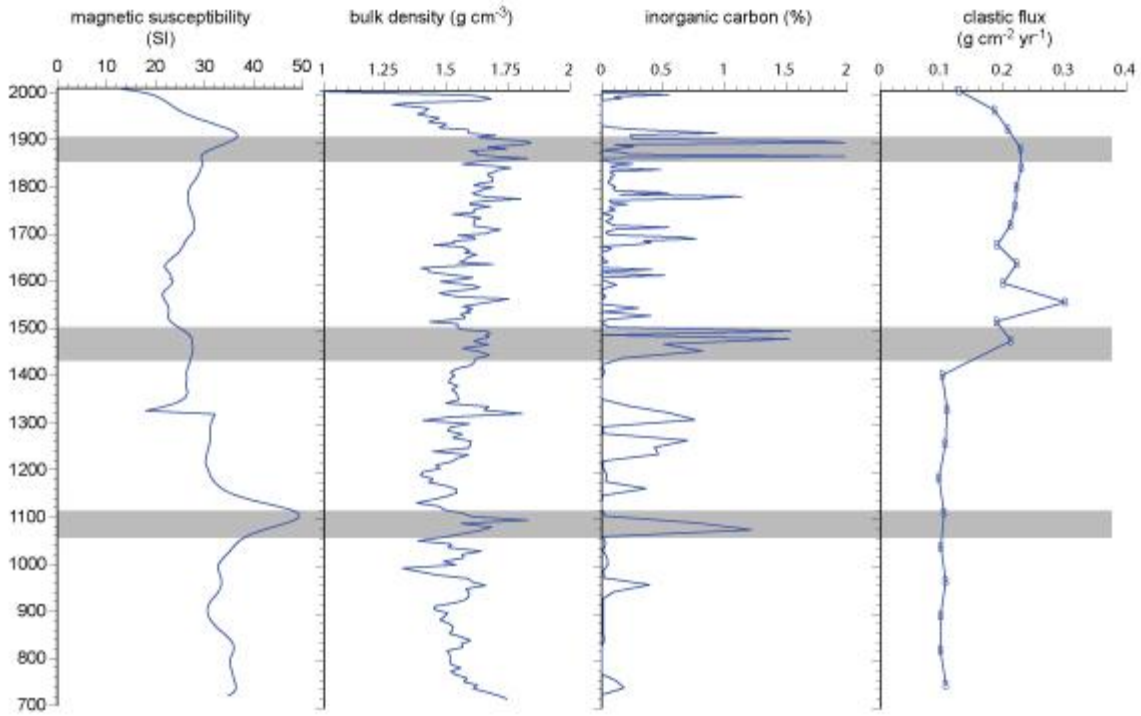

Figure 11. Plots of magnetic susceptibility, bulk density, % inorganic carbon, and clastic sediment flux through time. % inorganic carbon, bulk density, and clastic sediment flux track together and reflect changes in the input of allochthonous material to Grinnell Lake.

Glacial History based on Grinnell Lake Sediment Core

Evidence from tree rings, reconstructed sea levels, and dated moraines document a warm period termed the Medieval Warm Period which began as early as 800 *AD* (Cronin et al., 2004). Scientists agree that this warm period preceded the Little Ice Age however, the time separating the conclusion of the Medieval Warm Period and the beginning of the Little Ice Age is not well understood. Moraine evidence from the Canadian Rockies indicate the expansion of glacial ice about 1050-1150 *AD* (Leonard, 1986; Grove, 2001). Additionally, glacial activity in the coastal ranges of Alaska and adjacent Yukon Territory indicate two to three phases of glacial advances from 1100-1300 *AD* (Wiles et al., 2004; Barclay et al., 2009). However, temperatures derived from an oxygen isotope profile through a stalagmite in New Zealand suggest the Medieval Warm

Period persisted until about 1400 *AD* (Wilson et al., 1979). This interpretation was supported by a 1100-year tree ring record from New Zealand and studies from lake Ni-no-Megata and San-no-Megata in northeastern Japan (Cook et al., 2002; Kazuyoshi et al, 2010).

The absence of inorganic carbon coupled with relatively stable bulk density, magnetic susceptibility, and clastic sediment flux values from ~740-1090 *AD* reflect a limited input of allochthonous material and suggest that Grinnell Glacier did not exist during this period. This data supports the hypothesis of a warm climate initiated ~800 *AD* which persisted until at least ~1090 *AD*. However, the conclusion of this warm period and the transition to the cooler Little Ice Age is not easily deciphered from this study as peak inorganic carbon values at ~1090 *AD* and ~1450 *AD* may each reflect deposition of glaciagenic material. Initiation of the Little Ice Age in Glacier National Park is thought to have commenced ~1400 *AD* and persisted until ~1900 *AD* (Key et al., 2002). However, documented glacial advances in the Canadian Rockies ~1100 *AD* mark the beginning of the Little Ice Age in this region (Grove, 2001). Thus, large pulses of inorganic carbon in the Grinnell Lake record at ~1090 *AD* and ~1480 *AD* may each reflect the input of allocthonous material and represent possible periods of glacial expansion.

Tree ring records from the Columbia Ice Field record anomalously low temperatures ~1200 *AD*, ~1430-1500 *AD*, and ~1800-1900 *AD* (Fig. 12) (Luckman, 2000). These periods of reduced summer temperatures correspond to the three most significant increases of inorganic carbon in the Grinnell Lake record. Therefore, I suggest that the initiation of the Little Ice Age in Glacier National Park began ~1100 *AD*, earlier than has been previously documented.

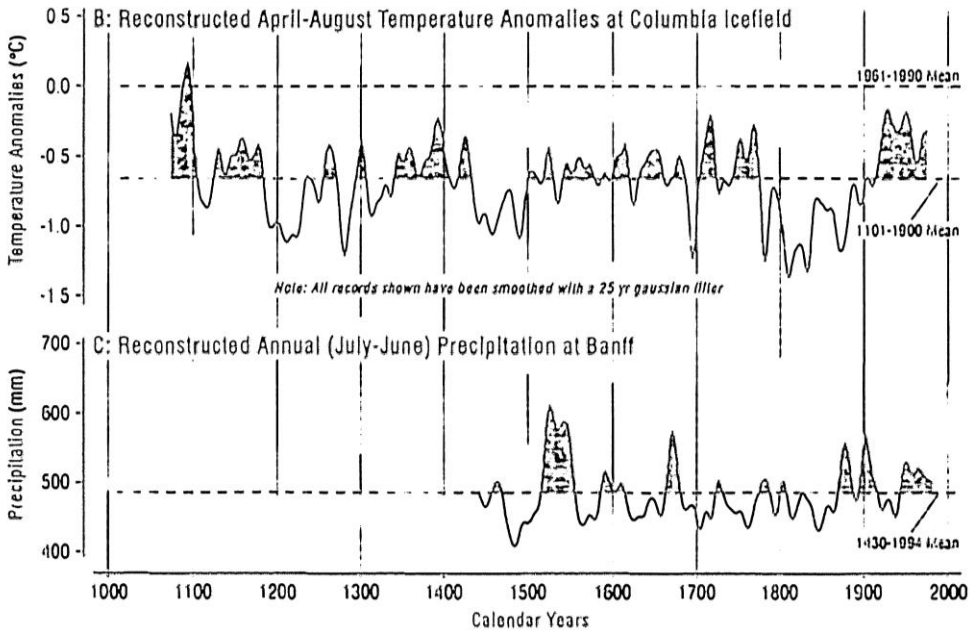

Figure 12: Comparison of reconstructed temperature (B) and precipitation records derived from tree rings in the Canadian Rockies. Maximum glacial extent occurred at the end of *AD* 19th century driven by cold and wet conditions (Figure from Luckman, 2000).

The Little Ice Age does not display a continuous period of cooling or glacial conditions. Colder conditions are variable over the past thousand years, and are punctuated by intermittent periods of warmth (Leonard, 1986; Bradley and Jones, 1993). Therefore, the apparent decrease in the inorganic carbon record from ~1110-1430 *AD* might represent a warm period within the Little Ice Age and reflect a time of little or no glacial expansion. A significant decrease in MS (46.7-22.3 m^3/kg) coincides with a gradual increase in wt % biogenic silica (0.12-0.41) during this time period suggesting that the climate was conducive for increased productivity. Rapid increases in clastic sediment flux and inorganic carbon ~1430 *AD* represent a return to a cool climate and glacial conditions. This interpretation is supported by tree ring records from the Columbia Ice Field (Fig. 12).

Clastic sediment flux, bulk density, and inorganic carbon all display increasing trends from ~1500-1900 *AD* and likely represent an extended period of glacial conditions. Peak inorganic carbon, bulk density, and magnetic suscpetibility values coincide with high clastic sediment flux data ~1900 *AD* and reflect the period of maximum glacial extent. The anomalously high clastic sediment flux value ~1550 *AD* coincides with low inorganic carbon values and may represent the deposition of material from a mass wasting event. Because the Grinnell Glacier erodes the Siyeh Limestone, the input of glaciagenic material would significantly increase both clastic sediment flux and inorganic carbon values simultaneously.

The Grinnell Glacier reached its maximum extent due to anomalously cold summer conditions. Temperature reconstructions from tree rings in the Columbia Ice Field indicate that from ~1770-1900 *AD*, summer temperatures were cooler than at another time during the past 1000 years. Additionally, moraine evidence from Glacier National Park suggests that most moraines (>80%) were deposited by the most recent advance in the mid-19th century suggesting that the climatic cooling of the mid-19th century produced glaciers that overran and destroyed moraines deposited by previous glacial advances (Carrara, 1989). This interpretation is also supported by Leonard (1986) who determined that periods of glacial advance and/ or of cold temperatures of a century or more duration are reflected in periods of persistently high downvalley sedimentation. Leonard (1986) found sedimentation rates were highest in glacially-fed Hector Lake, Alberta ~1850 *AD* (Fig. 13).

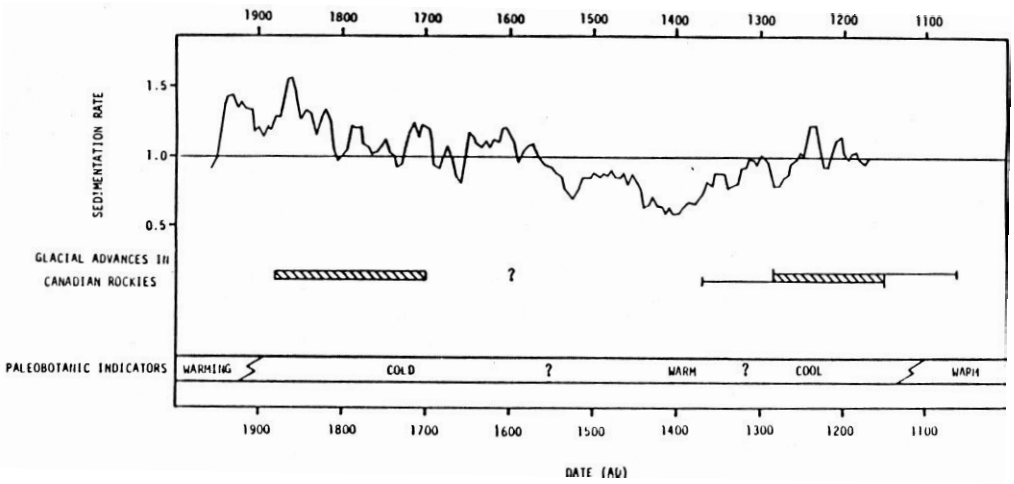

Figure 13. Composite sedimentation rate curve for glacial-fed Hector Lake (Canadian Rocky Mountains) compared with glacial history and paleobotanic indicators of climate in the Canadian Rockies over the past 900 years. Periods of increased sedimentation rates coincide with both Late Holocene glacial advances and occur during cool climates (Figure from Leonard, 1986).

Rapid decreases in % inorganic carbon, bulk density, magnetic susceptibility and clastic sediment flux from ~1900 *AD* to the present mark the end of the Little Ice Age and the beginning of rapid glacial retreat. The Grinnell Glacier was first visited in 1885 *AD* by George Bird Grinnell. Mr. Grinnell fell in love with the glacier and returned each year for the next several decades and was also among the early explorers to advocate the establishment of Glacier National Park. Grinnell Since it was first observed in 1887 *AD*, the Grinnell Glacier has significantly diminished in area. These changes are well documented thanks to the photographs taken by Mr. Grinnell in 1887 *AD* and his later photographs taken from the same locations. These early photographs coupled with extensive mapping of the Grinnell Glacier which, began in 1900 *AD*, illustrate the changes in the glacier's extent over the past century (Johnson, 1980). These data were used to generate a map of the Grinnell Glacier that suggests the glacier began to retreat ~1850 *AD*, about 50 years prior to interpretations made in this report. Additionally, Key et al. (2009) have demonstrated that the rate of recession of the Grinnell Glacier has not been

constant through time receding about 6 m a^{-1} from 1859-1920 *AD* and at an average rate of 15 m a^{-1} between 1920-1946 *AD*. Figure 14 compares proxy indicators of glacial extent from this Grinnell Lake sediment core to known Grinnell Glacier terminus positions. From ~1850 *AD* to the present, clastic sediment flux values decrease. Three distinct peaks in inorganic carbon at 1870 *AD*, 1900 *AD*, and 1920 *AD* likely represent the input of glacial deposits due to paraglacial processes such as fluvial reworking. Despite increased temperatures post-1850 *AD*, biogenic silica values remain relatively low until 1890 *AD* when they begin to increase more rapidly. Similarly, organic carbon values decrease from 1850-1940 *AD* before they begin to increase. These finding may be due to the continued influx of glaciagenic debris to Grinnell Lake increasing the turbidity of the water thus lowering the amount of available sunlight and inhibiting productivity. The findings in this report are consistent with interpretations from previous studies suggesting that paraglacial processes limit the resolution of glacial chronologies based on lacustrine sediment to about a century (Church and Ryder, 1972). Key et al. (2009) suggest that the Grinnell Glacier retreated fastest from 1920-1946 however the absence of inorganic carbon, the decrease in clastic sediment flux and bulk density, coupled with increases in biogenic silica and organic carbon indicates that most loose glaciagenic material had been reworked, transported, and deposited in the Grinnell Lake by this time.

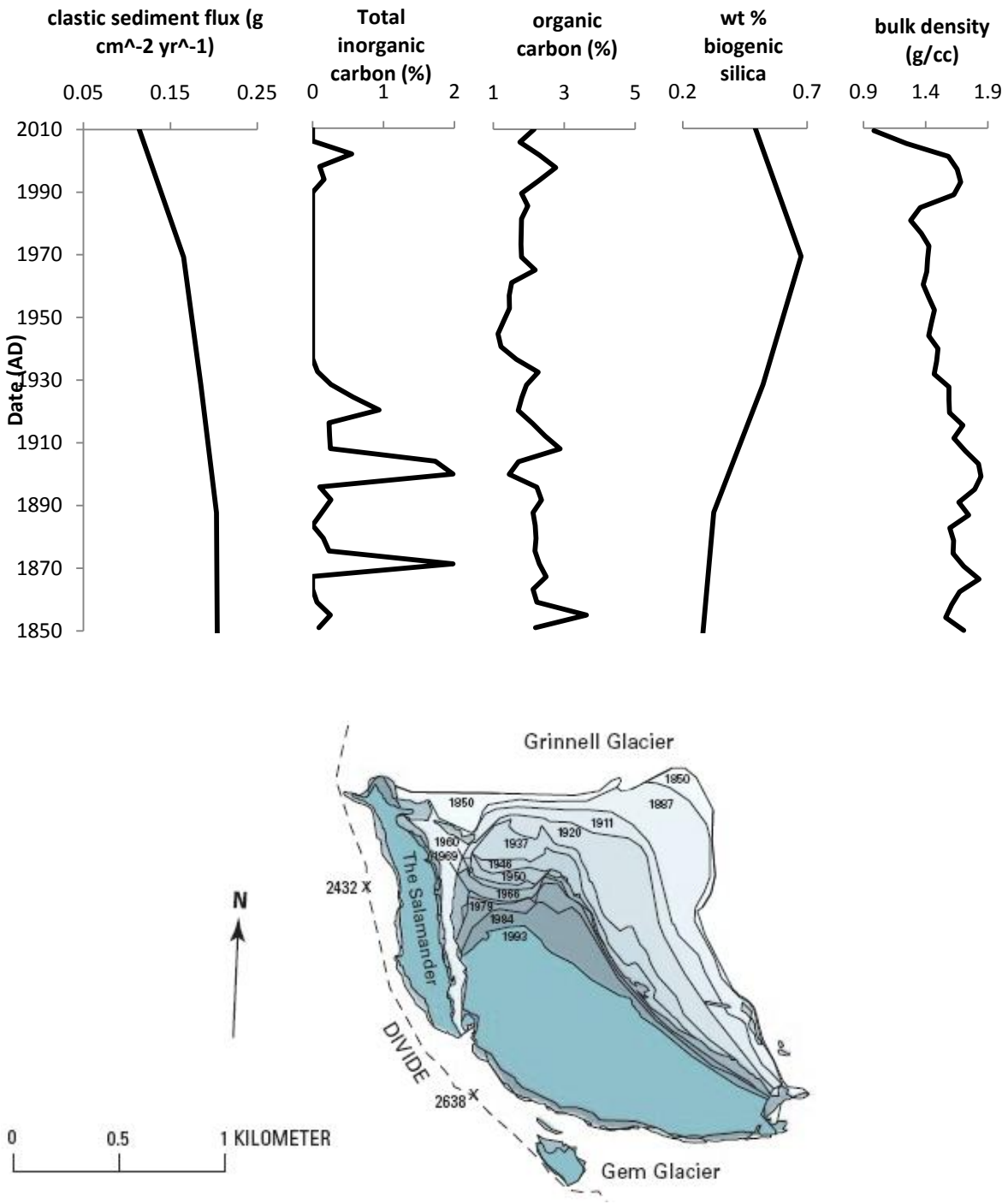

Figure 14. Downcore plots for clastic sediment flux, % inorganic carbon, % organic carbon, wt % biogenic silica, and bulk density since 1850 compared to know terminus positions of the Grinnell Glacier since 1850. Notice that the Grinnell Glacier first retreats in 1850 however pulses of glaciagenic material (indicated by peak % inorganic carbon values and relatively high bulk density values) persist until about 1920.

Enhanced Productivity Implications

Despite all of the evidence documenting glacial fluctuations during the Little Ice Age, these data cannot be directly translated into quantitative measures of temperature and/or precipitation. Periods of glacial expansion are times of positive mass balance but the specific mix of temperature and precipitation inputs that result in mass balance changes is difficult to interpret. Additionally, the glacier response to these climate factors is often lagged, and is modulated by the characteristics and setting of individual glaciers (e.g., size, topography) (Luckman, 2000). However, by supplementing a glacial record with regional tree-ring and in situ carbon and nitrogen isotope data, it is possible to estimate the relative inputs of temperature and precipitation and their effects of individual glaciers.

Data from this study document relative increases in organic carbon and biogenic silica (Fig. 15), coincident with a decrease in C/N ratios from ~1640-1920 *AD* (Fig. 8). This period reflects a time of significant glacial expansion, which was interpreted to be related to reduced temperatures. Times of decreased temperatures are often related to periods of reduced productivity however that is not the case in Grinnell Lake. This observation may be explained using carbon and nitrogen isotopes. Figure 9 shows plots of carbon and nitrogen isotopes through time. $\delta^{13}C$ becomes more enriched through time however $\delta^{15}N$ values shift sporadically and demonstrate no clear trend. Carbon isotopes in sedimentary organic matter may be used as indicators of productivity becoming enriched with increasing productivity and depleted with decreasing productivity (Hodell & Schelske, 1998, O'Reilly et al., 2003).

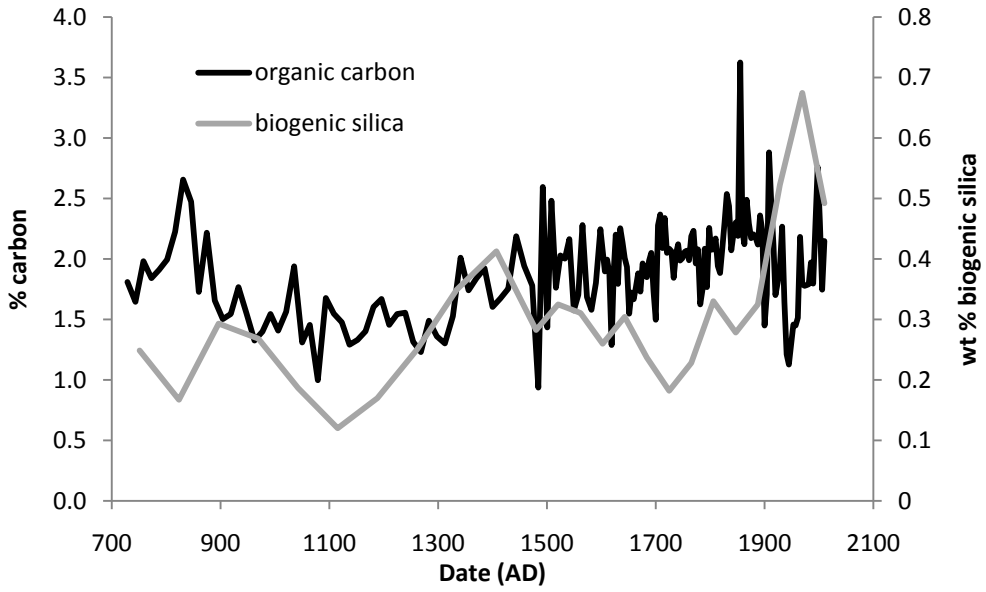

Figure 15. Plots of organic carbon and biogenic silica. Both track together because they are each proxy indicators of productivity.

O'Reilly et al. (2003) analyzed sediment cores from Lake Tanganyika, Africa and attributed the lakes decrease in productivity to rising temperatures. They suggest that during the cool windy season, strong winds tilt the thermocline thus inducing upwelling of nutrient-rich waters. Additionally, cooling weakens the thermocline further promoting the entrainment of nutrients from deeper water. These mixing events provide an important source of limiting nutrients (N, P) to the surface waters and increase the lakes productivity (O'Reilly et al., 2003). Unlike Lake Tanganyika, Grinnell Lake is well mixed and thus not permanently thermally stratified. However, decreased temperatures coupled with increased wind velocities may have weakened what little thermocline Grinnell Lake has thus promoting the upwelling of nutrients and increasing productivity. The largest increase in organic carbon and biogenic silica occurs from ~1650-1900 *AD*, coincident with the timing of maximum glacial extent. Temperatures during this period may have been colder than at any other point in the past 1200 years, thus an extremely weak thermocline may have induced increased productivity.

The increased accumulation of nutrients from the atmosphere may have also caused the observed increase in productivity. Nitrogen and phosphorous are the elements in greatest demand by phytoplankton and thus their concentrations are important controls on productivity. Nitrogen can be incorporated in rain through the volatization of ammonia, nitrification and denitrification of soils, and anthropogenic sources (Cohen, 2003). Wiles et al. (2004) and Barclay et al. (2009) suggest the middle to late-Little Ice Age advances were closely related to increased alpine precipitation. Therefore, Grinnell Lake's increase in productivity from ~1650-1900 *AD* may be related to enhanced rainfall, thus increasing the concentration of important nutrients such as nitrogen in the lake and promoting productivity.

Thus, increased rates of productivity coupled with an enrichment in $\delta^{13}C$ are attributable to increased nutrient concentrations related to two factors. Colder temperatures coupled with high winds from ~1650-1900 *AD* may have weakened the thermocline and promoted the upwelling of deep water nutrients. However, since Grinnell Lake is well-mixed, this affect might be minimal. Additionally, nitrogen concentrations, an important control on productivity, may have increased in Grinnell Lake due to enhanced precipitation.

Based on the sediment properties of Grinnell Lake, ~1650-1900 *AD* represented a period of increased glacial activity during which the Grinnell Glacier reached its maximum extent ~1900 *AD*. This period also coincides with an observed increase in the lakes productivity which may be attributed to higher nutrient concentrations related to colder and wetter conditions. Thus, increased productivity and $\delta^{13}C$ values record a cold and wet climate and it is this combination that drove the Grinnell Glacier to its maximum extent in 1900 *AD*.

CONCLUSION

A ~1.2 kyr lacustrine sediment record extracted from Grinnell Lake in the northern Rocky Mountains of the United States provides a multi-proxy climate and glacial record in the Late Holocene. Glacial-interglacial fluctuations were documented and correlated with previously constructed records in regional geographical locations demonstrating the usefulness of clastic sediment flux to alpine lakes as a proxy indicator for the extent of regional ice cover (Rodbell et al., 2008; Leonard, 1986). Changes in clastic sediment flux were coincident with changes in % inorganic carbon and bulk density and documented the input of glaciagenic material into the lake basin. Over timescales of decades to centuries, downvalley sedimentation rates are controlled by glacial activity upvalley (Leonard, 1986), therefore periods of increased clastic sediment flux were interpreted to reflect glacial advances. An increase in inorganic carbon ~1090 *AD* represents the initiation of the Little Ice Age and marks the beginning of glacial conditions. The period from ~1100-1400 *AD* is relatively stable however a rapid increase in clastic sediment flux and inorganic carbon ~1430 *AD* documents a change to a cooler climate and a return to glacial conditions. Peak clastic sediment flux values ~1900 *AD* reflect the maximum glacial extent of the Grinnell Glacier.

The glacial record constructed from the Grinnell Lake sediment core was successful in demonstrating the usefulness of lake sediments for glacial reconstructions. However, an additional dataset that would be useful to correlate with the clastic sediment flux record is determining the presence of dolomite. Since the only source of dolomite in the catchment is overlain by the Grinnell Glacier, periods of glacial expansion and thus increased scour are likely to increase the concentration of dolomite in downvalley glacial-fed lakes. By comparing a record of dolomite to the clastic sediment flux dataset, it may be possible to distinguish clastic

sediment delivered by enhanced glacial erosion from sediment derived from the surrounding hillslopes.

On comparison with regional records from the Rocky Mountains of the United States and the Canadian Rocky Mountains, it appears that the Little Ice Age was driven by similar climate forcing mechanisms. This prolonged cold period is punctuated by intermittent periods of warmth and is not globally synchronous. Records from the Cordillera Blanca, in northern Peru (Tonry, 2010), European Alps (Fagan, 2000), and even Patagonia (Grove, 1988) display evidence of a sustained cold climate during the Late Holocene however, the precise timing does not correspond. The continued compilation of geographically diverse climate records from the Little Ice Age period can only help to analyze changes in the global climate. Understanding the timing and magnitude of this cold period may help determine small scale forcing mechanisms that are driving climate change, and how these changes might propogate globally.

REFERENCES

Alley, R.B. (2000) The Younger Dryas cold interval as viewed from central Greenland. Quaternary Science Reviews 19, 213-226.

Alley, R.B., Bond, G., Chapellaz, Glapperton, C., Del Genio, A., Keigwin, L., Peteet, D. (1993a) Global Younger Dryas, EOS 704, 587-589.

Anderson, L., Finney, B. P., Shapley, M. D. (2011) Lake carbonate d18O records from the Yukon Territory: Little Ice Age moisture variability and patterns, Quaternary Science Reviews 30, 887-898.

Barclay, D. J., Wiles, G. C., Calkin, P. E. (2009) Holocene glacier fluctuations in Alaska, Quaternary Science Reviews 28, 2034-2048.

Benedict, J. B. (1973) Chronology of Cirque Glaciation, Colorado Front Range, Quaternary Research 3, 584-599.

Benn, D. I., and Evans, D. J.A. Glaciers and Glaciation. New York, NY: Oxford University Press Inc., 1998.

Bradbury, J.P., Bezrukova Y.V., Chernyaeva G.P., Colman S.M., Khursevich G., King J.W., Likoshway Y.V., (1994) A synthesis of post-glacial diatom records from Lake Baikal, Journal of Paleolimnology 10, 213-252.

Bradley, R.S. *Quaternay Paleoclimatology: Methods of Paleoclimatic Reconstruction*. Winchester, MA: Allen & Unwin Inc., 1985. 47-85.

Bradley, R.S. and Jones, P.D. (1993) 'Little Ice Age' summer temperature variations: their nature and relevance to recent global warming trends, Holocene 3, 367-376.

Carrara, P. E. U.S. Geological Survey. *Late Quaternary Glacial and Vegetative History of the Glacier National Park Region, Montana*. Denver, CO: United States Government Printing Office, 1989.

Church, M., and Ryder, J.M. (1972) Paraglacial sedimentation: a consideration of fluvial processes conditioned by glaciations, Geological Society of America Bulletin 83, 3059-3072.

Corbett, L.B., and Munroe, J.S. (2010) Investigating the influence of hydrogeomorphic setting on the response of lake sedimentation to climatic changes in the Uinta Mountains, Utah, USA, J. Paleolimnol 44, 311-325.

Davis, P. T., Osborn, G. (1987) Age of pre-neoglacial cirque moraines in the central North American Cordillera, Géographie physique et Quaternaire 41, 365-375.

Demaster, D. J., (1981) The supply and accumulation of silica in the marine environment, Geochimica et Cosmochimica Acta 45, p. 1715-1732.

Fagan, B. (2000) The Little Ice Age: How climate made history, 1300-1850. New York: Basic Books.

Grove, J.M. (2001) The initiation of the "Little Ice Age" in regions round the North Atlantic, *Climate Change* 48, 53-82.

Grove, J.M. (1988) *The Little Ice Age*, Methuen, London.

Johnson, A. (1980) Grinnell and Sperry Glaciers, Glacier National Park, MT – A record of vanishing ice. Geological Survey Professional Paper.

Hallet, B., Hunter L., Bogen, J. (1996) Rates of erosion and sediment evacuation by glaciers: a review of field data and their implications, Global and Planetary Change 12, 213-235.

Hasnain, S. (1996) Factors controlling suspended sediment transport in Himalayan glacier meltwaters, Journal of Hydrology 181, 49-62.

Hodell, D. A., Schelske, C. L. (1998) Production, sedimentation, and isotopic composition of organic matter in Lake Ontario, Limnol. Oceanogr. 43, 200-214.

Horodyski, R. J., (1983) Sedimentary Geology and Stromatolites of the Middle Proterozoic Belt Supergroup, Glacier National Park, Montana, Precambrian Research 20, 391-425.

Karlen, W. (1981) Lacustrine sediment studies: A technique to obtain a continuous record of Holocene glacier variations, Geogr. Ann. 63 A: (3-4), 273-281.

Key, C. H., Fagre, D. B., Menicke, R. K. (2002) Glacier Retreat in Glacier National Park, Montana, in Krimmel R.M., eds., Glaciers of North America-Glaciers of the Conterminous United States, 365-375.

Leonard, Eric. "Glaciological and climatic controls on lake sedimentation, Canadian Rocky Mountains." *Zeitschrift Fur Gletscherkunde Und Glazialgeologie*. (1985): 35-42.

Leonard, E. M. (1986) Use of Lacustrine Sedimentary Sequences as Indicators of Holocene Glacial History, Banff National Park, Alberta, Canada, *Quaternary Research* 26, 218-231.

Licciardi, J.M., Clark, P.U., Brook, E.J., Elmore, D., Sharma, P. (2004) Variable responses of western U.S. glaciers during the last deglaciation, Geology 32, 81-84.

Luckman, B. H. (1993) Glacier fluctuations and tree-ring records for the last millennium in the Canadian Rockies, Quaternary Science Reviews 12, 441-450.

Luckman, B., (2000) The Little Ice Age in the Canadian Rockies, Geomorphology 32, 357-384.

Luckman B.H., and Osborn, G.D. (1979) Holocene glacier fluctuations in the middle Canadian Rocky Mountains, Quaternary Research 11, 52-77.

MacGregor, K. R., Riihimaki, C. A., Myrbo, A., Shapley M.D., Jankowski, K. "Geomorphic and climatic change over the past 12,900 years at Swiftcurrent Lake, Glacier National Park, Montana, USA." *Quaternary Research*. (2010)

Mann, M.E., Bradley, R.S., Hughes, M.K. (1999) Northern Hemisphere temperatures during the past millennium: inferences, uncertainties, and limitations, Geophys. Res. Lett. 26, 759-762.

O'Reilly, C. M., Alin, S. R., Plisnier, P. R., Cohen, A. S., Mckee, B. A. (2003) Climate change decreases aquatic ecosystem productivity of Lake Tanganyika, Africa, Nature 424, 766-768.

Østrem, G. (1975) Sediment transport in glacial meltwater streams. In: Jopling, A.V., McDonald, B.C. (Eds.), Glaciofluvial and Glaciolacustrine Sedimentation, Special Publication 23. Society of Economic Palaeontologists and Mineralogists, Tulsa, OK, pp. 101-122.

Qui, L., Williams, D.F., Gvordzdkov, A., and Karabanov, E. (1993). Biogenic silica accumulations and paleoproductivity in the northern basin of Lake Baikal during the Holocene. Geology 21, 25-28.

Ritter, D. F., Kochel, R. C., Miller, J. R. Process Geomorphology. 4. Long Grove, IL: Waveland Press, Inc., 2002.

Rodbell, D. T., Seltzer G. O., Mark, B. G., Smith, J. A., Abbott, M. A. (2008) Clastic Sediment flux to tropical Andean lakes: records of glaciation and soil erosion, *Quaternary Science Reviews*. 27, 1612-1626.

Rosenbaum, J. G., and Reynolds, R. L. (2004) Record of Late Pleistocene glaciation and deglaciation in the southern Cascade Range. II. Flux of glacial flour in a sediment core from Upper Klamath, Oregon *Journal of Paleolimnology* 31, 235-252.

Rosenbaum, J. G., and Heil, C. W. (2009) The glacial/deglacial history of sedimentation in Bear Lake, Utah and Idaho, in Rosenbaum J.G., and Kaufman D.S., eds., Paleoenvironments of Bear Lake, Utah and Idaho, and its catchment: Geological Society of America Special Paper 450, 247-261.

Seltzer, G.O., Rodbell, D.T., Abbott, M. (1995) Andean glacial lakes and climate variability since the last glacial maximum: Bull. Inst. Fr. Etudes andines, 24 (3), 539-549.

Sharp, Z. Princles of Stable Isotope Geochemistry. Upper Saddle River, NJ: Pearson Prentice Hall, 2007.

Tonry, S. 2010, A continuous record of lateglacial and Holocene paleoclimatic change from Laguna Yanacocha sediment cores, Cordillera Blanca, Peru. B.S. ed. Schenectady, NY: Union College.

Wiles, G. C., D'Arrigo, R. D., Villalba, R., Calkin, P. E., Barclay, D. J. (2004) Century-scale solar variability and Alaskan temperature change over the past millennium, Geophysical Research Letters 31.

APPENDICES

Appendix 1. XRD data

Running depth (cm)	Minerals present
0	quartz, dolomite, graphite-2H, ankerite, calcite
5	quartz, calcium iron oxide, graphite, stishovite, magnetite
10	quartz, dolomite
15	quartz, montmorillonite-14A, dolomite, spinel, syn (MgAl2O4), ankerite, anatase (TiO2), Montmorillonite-15A
20	quartz, montmorillonite-14A, ankerite, clinochlore, dolomite, illite, lime (CaO), spinel, halite, montmorillonite-15A
25	quartz, dolomite, ankerite
30	quartz, clinochlore, montmorillonite-14A, dolomite, stishovite, spinel, zironolite, montmorillonite-15A
35	quartz, stishovite, ulvospinel (Fe2TiO4), dolomite, halite, ankerite, calcium sulfate, calcite, calcium iron oxide
40	quartz, dolomite, graphite, halite
45	quartz, halite,calcium iron oxide (Ca3Fe15O25), ankerite, dolomite, calcium iron oxide (CaFeO3)
50	quartz, dolomite, halite, spinel
55	quartz, dolomite, zirconolite, montmorillonite-14A
60	quartz, montmorillonite-14A, clinochlore, dolomite, ankerite, montmorillonite-15A
65	quartz, dolomite, ankerite, calcite
70	quartz, ankerite, dolomite
75	quartz, spinel, ankerite, dolomite, rutile (TiO2)
80	quartz, lime (CaO), illite, graphite, dolomite, ankerite, stishovite
85	quartz, dolomite, ankerite, calcium iron oxide, graphite
90	quartz, montmorillonite-14A, illite, clinochlore,ankerite, spinel, dolomite, Montmorillonite-15A
95	quartz, dolomite, spinel
100	quartz, anatase (TiO2), dolomite, (calcite,magnesium (Ca,Mg)CO3), ankerite
105	quartz, zirconolite, stishovite, ankerite, halite, dolomite
110	quartz, dolomite, ankerite, stishovite,graphite
115	quartz, dolomite

Appendix 2. Grinnell Lake core logs

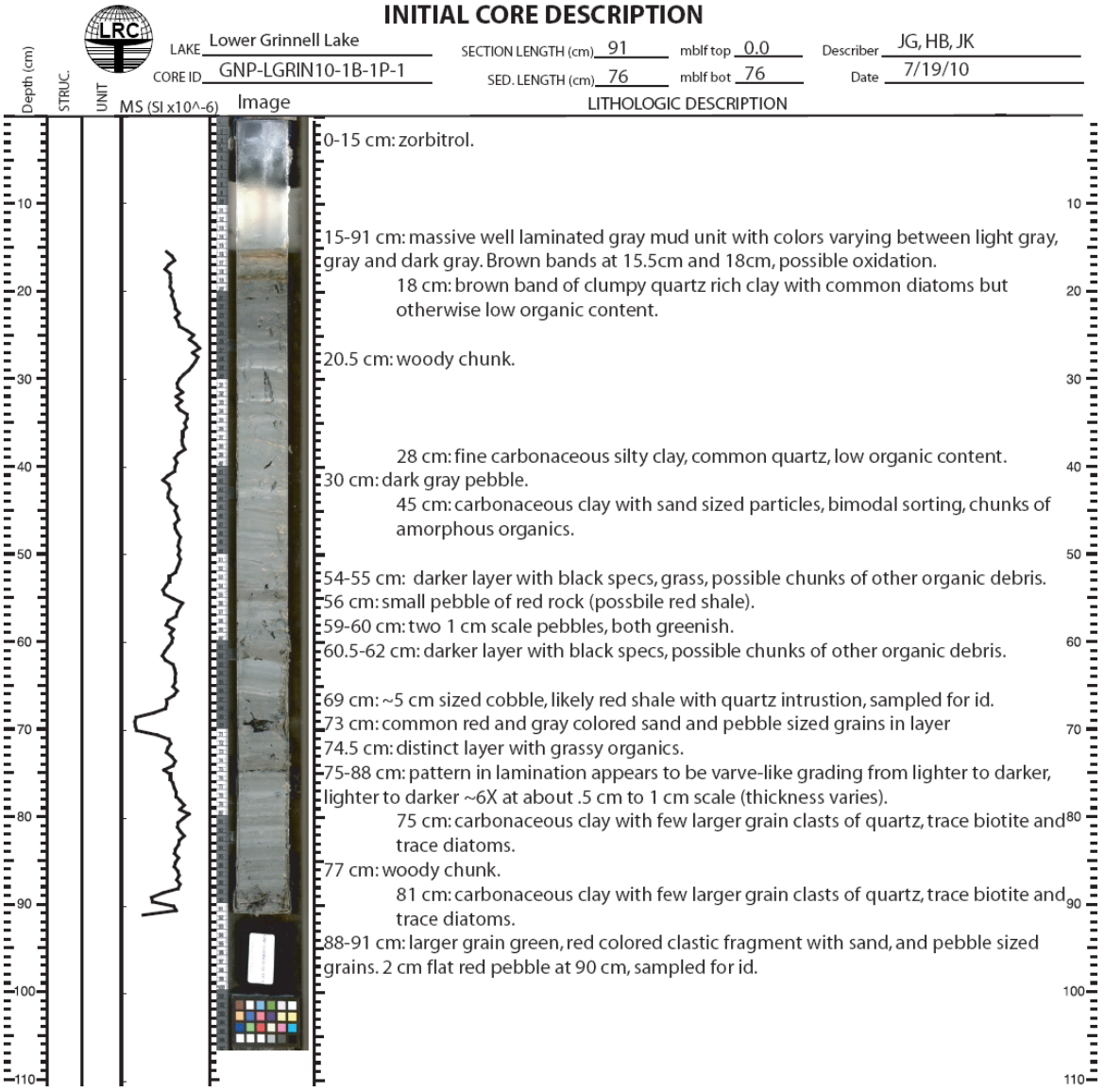

INITIAL CORE DESCRIPTION

LAKE Lower Grinnell Lake
CORE ID GNP-LGRIN10-2B-1
SECTION LENGTH (cm) 143 mblf top ###.# Describer HB, JK
SED. LENGTH (cm) 143 mblf bot ###.# Date 7/19/10

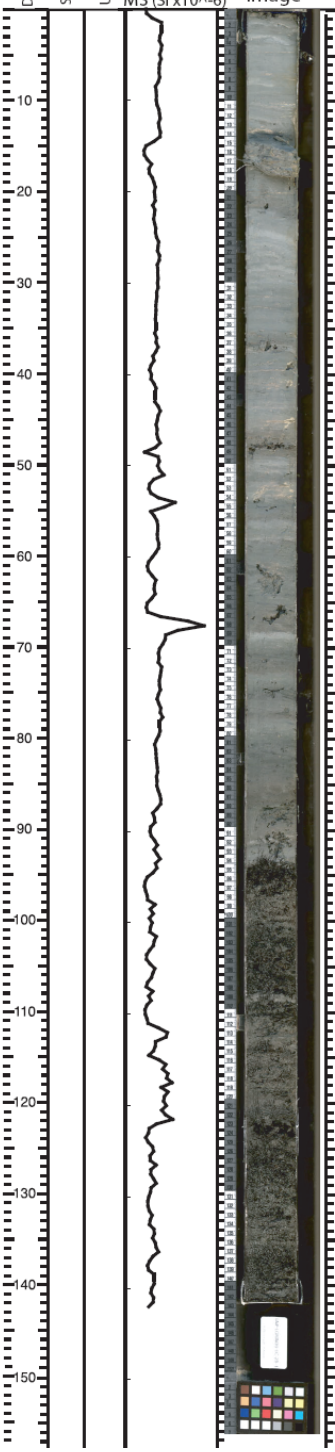

LITHOLOGIC DESCRIPTION

0-94 cm: massive laminated gray mud unit with colors varying between light gray, gray and dark gray. color changes are subtle and varve-like patterns are not clear.

14-17.5 cm: large red cobble (~6 cm long and ~3 thick) beneath which the existing layers seems to have been deformed from the dropping of the cobble and planar lamination resumes at ~26 cm.

48-49 cm: darker band with pebbles and some grassy organics.

69 cm: distinct lighter band.
73 -80 cm: alternating light and dark bands with diffuse boundaries.

86-88 cm: darker gray layer with black specs.

92 cm: light gray band
94 cm: unit of coarse grained sand and abundant woody organic debris. Sand particles of various colors- red, white, green and grey. Layers unidentified coniferous tree needles PINE NEEDLE (cm scale) with overlying sand and mud layers (result of different settling velocities).

123-124 cm: black woody chunk.

Note: correlates with GNP-LGRIN10-1A-1P-1 and GNP-LGRIN10-1A-2B-1.

Appendix 3. Procedure for extraction and analysis of biogenic silica

Procedure
See procedure outlined at http://www1.union.edu/rodbelld/biogenicsilica.htm

Analysis

Analysis of samples is by ICPMS. This machine detects small concentrations of elements. Samples were diluted by a factor of 22 (1) in order to fall within the machines detection limits. In this study, we identified the concentrations of silica, aluminum, and vanadium. Vanadium was selected as a control and used in a diluting solution (2) because it was virtually absent from the samples. Constant concentrations of vanadium indicate that the machine is running properly. In addition, aluminum was examined because any concentration of it in solution suggests it had dissolved from the clastic alumino-silicate component in the sample. When run through the ICPMS, samples were compared to blanks (3) and standards (4) containing known concentrations of Si and Al standards. Silica and aluminum concentrations were determined from each sample at the 2, 3, 4, and 5 hour extractions and plotted in excel. In order to obtain the total biogenic silica in the original sample, a best-fit trendline was fit to the silica data and extrapolated back to the y-axis. The intersection of the best-fit line with the y-axis represents the concentration of biogenic silica (ppb) in the sample.

However, samples analyzed on the ICPMS were diluted by 22 times and therefore the biogenic silica concentration data is also diluted and must be multiplied by 22 to reflect the amount of biogenic silica in the original sample. Initial concentrations (y-intercept equivalent) were in units of ppb and converted to ppm by dividing the initial concentration by 1000. Next, the silica concentration (ppm) was divided by the (mass of the original sediment sample/1000) to determine the mass of Si per gram of sample (Si concentration (ppm)/(original sediment mass/1000))= micrograms Si/ gram of sample. However, in this study we are looking for biogenic silica which has a chemical formula of SiO_2. To account for these two oxygens, micrograms Si/ gram of original sample value was multiplied by 2.14, that is the atomic mass of SiO2 divided by the mass of silica (60/28). The result of this calculation is in units of (micrograms bSiO2/gram of sample). This value was then converted to bSiO2 weight percent by dividing (micrograms bSiO2/gram of sample) result by 10000 ((micrograms bSiO2/gram of sample)/100000). Lastly, in order to use this value in the clastic sediment flux equation, the bSiO2 weight percent was divided by 100 and thus converted to a decimal fraction.

1) Dilution Factors

a) During extraction procedure, at 2, 3, 4, and 5 hours, 1 ml of solution is drawn off and placed into a vial. Then, 1 ml of DI water is added to the vial thus diluting the sample and making it half as concentrated.

b) Next, 0.5 ml of sample from each vial (already cut in half) is extracted, placed into another vial, and then 5 ml of diluting solution is added (5.5/0.5=11).

c) Taking into account both diluting factors (2/1=2, 5.5/0/5=11) the total dilution was calculated (2*11=22).

2) Dilution Solution

a) Run a sample and pick an element with very low concentration to be used in the diluting solution (Vanadium in this study)
b) Concentration of vanadium stock solution = 999 µg/ml = 1 µg/l, looking for a dilution solution with 20 PPB vanadium
c) 0.001 ml of vanadium/ 1 L water = 1 PPB vanadium, so,
0.02 ml vanadium/ 1L water = 20 PPB vanadium

3) Blank
a) During extraction procedure, at 2, 3, 4, and 5 hours, place 1 ml of NaOH (heated at 85˚C) in a tube, and add 1 ml of DI water. At the end, the tube will contain 8 ml of solution, 4 ml NaOH + 4 ml DI water.
b) Blank must have a dilution factor of 11 because of the 11X dilution in step 1b (above)
c) 40 ml diluting solution + 4 ml NaOH + water (8 ml NaOH + water cut in half) = 44 ml blank
d) 44 ml blank / 4 ml NaOH + water = 11

4) Standards – silica and aluminum (100 PPB and 500 PPB)
100 PPB STD:
Si stock STD = 1000 µg/ml = 1000 µl/ml, 1 mg/ 1L= 1 ppm
   a) 1 ml/1 L = 1 ppm
      a. 100 ppb = 0.1 ppm
      b. 0.1 ml Si/ 1 L solution = 100 ppb
   b) For 100 ppb:
      a. 0.1 mg/ 1000 ml = x/44 ml
      b. Cross multiply: 1000x = 4.4
      c. x = 0.0044 ml of Si stock solution or 4.4 µl of Si stock solution in 44 ml of blank
   c) Aluminum stock standard is also 1000 µg/ ml, 4.4 µl of Al stock solution in 44 ml of blank = 100 ppb Al STD
   d) to maintain the same volume, remove 8.8 µl of blank from 44 ml total **before** adding 4.4 µl of Si and 4.4 µl of Al stock solution
   e) Therefore, add 4.4 µl of Si and 4.4 µl of Al stock solution to 39.912 ml blank

5) Standards – silica and aluminum
500 ppb STD:
   a) 500 ppb STD is simply 5X larger than 100 ppb STD
   b) 4.4 µl * 5 = 22 µl
   c) Therefore, a standard consisting of 500 ppb of Si and Al, must have 22 µl of both Si and Al
   d) To maintain the same volume, remove 44 µl of from 44 ml blank total **before** adding 22 µl of Si and 22 µl of Al